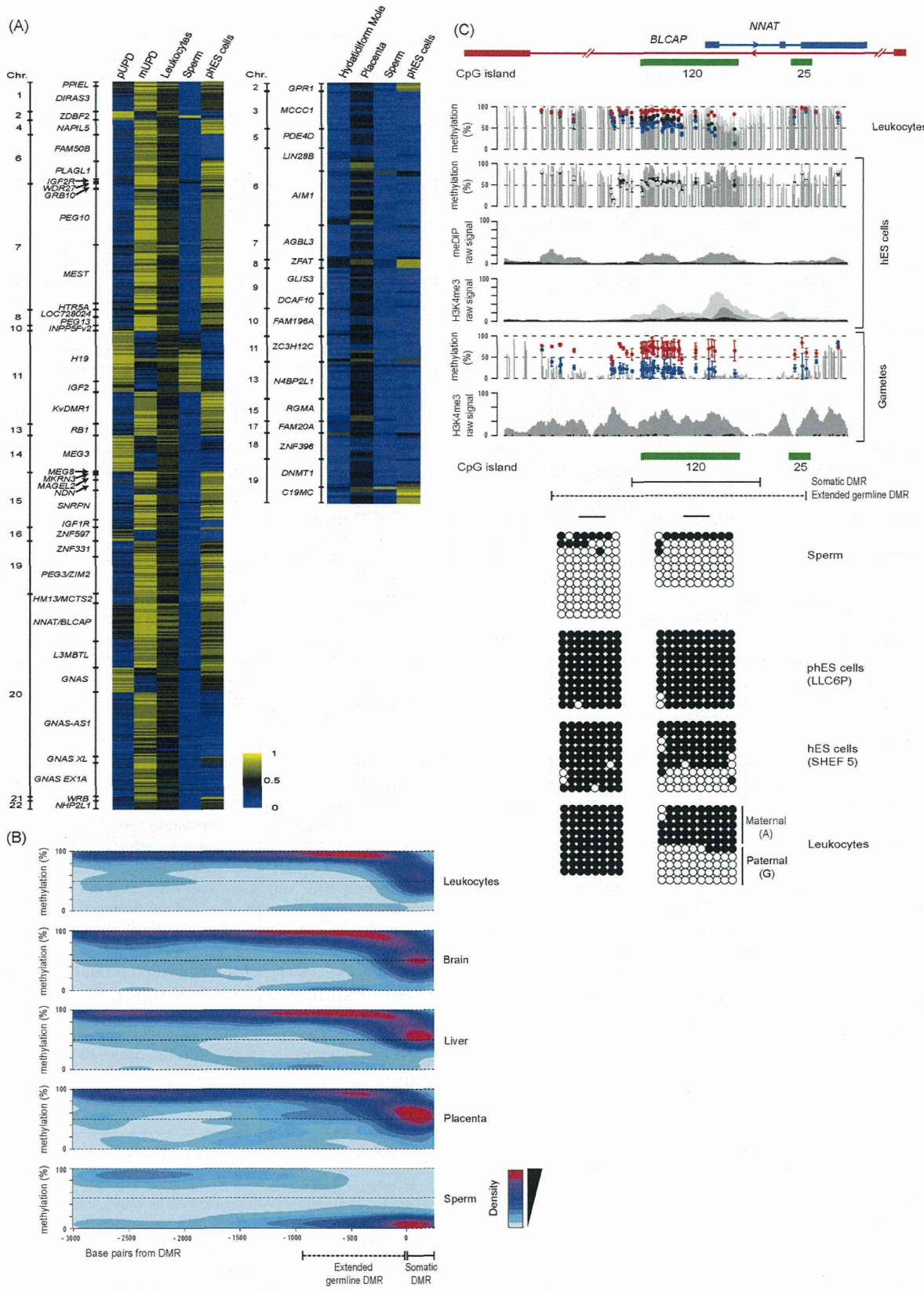

Figure 5. (Legend on next page)

BeadChip arrays to identify imprinted loci (Nakabayashi et al. 2011). All new regions of ubiquitous imprinted methylation identified in the current screen are associated predominantly with type II Infinium probes and were not present on previous array platforms. Of the placental-specific DMRs, only those associated with *DNMT1, AIM1,* and *MCCC1* have been previously described (Yuen et al. 2011; Das et al. 2013). Intriguingly, the somatic promoter of *Dnmt1* is differentially methylated between sperm and oocytes but is lost during preimplantation development (Smallwood et al. 2011; Kobayashi et al. 2012). Two of these placental-specific DMRs are associated with type I Infinium probes and were previously discovered using the Infinium HumanMethylation27 BeadChip arrays with DNA derived from diandric and digynic triploid placental samples (Yuen et al. 2011).

Our data provide the first direct evidence in humans that the differential methylation associated with imprinted genes is dynamically regulated upon fusion of the gametes at fertilization. Most maternally methylated DMRs are surrounded by regions of complete methylation in both gametes, and as in mice, the DMRs are clearly observed as unmethylated islands in the sperm genome. These unmethylated intervals are often more extensive in sperm compared to somatic tissues, suggesting that resizing occurs during embryonic transition. It was recently reported that nucleosomes are retained at specific functional regions in sperm chromatin and are refractory to protamine exchange (Hammoud et al. 2009). These sperm-derived histones are enriched for H3K4me3, a permissive modification that is mutually exclusive with DNA methylation, implicating these H3K4me3 regions in the maintenance of the unmethylated state in the male germline.

Imprints are distinguishable from other forms of gametic methylation as they survive the reprogramming that initiates immediately upon fertilization (Smallwood et al. 2011; Kobayashi et al. 2013; Proudhon et al. 2012). By comparing the profiles of sperm, phES, and conventional hES cells along with somatic tissues, we present evidence that most maternally methylated DMRs are not completely refractory to reprogramming, as highlighted by the substantial resizing of the paternally derived unmethylated alleles. These data are consistent with the notion that the cores of imprinted DMRs are protected from Tet-associated demethylation by recruiting heterochromatic factors such as ZFP57 and DPPA3 (also known as STELLA or PGC7) (Nakamura et al. 2007; Li et al. 2008). Similar mechanisms could also act to protect the core of the unmethylated paternal alleles from methylation.

A search for the mouse ZFP57 recognition sequence ($TGCC^{met}GC$) identified numerous binding sites within the ubiquitous imprinted DMRs that may be involved in protecting methylation during preimplantation reprogramming (Quenneville et al. 2011). It is currently unknown if this hexonucleotide motif is bound by ZFP57 in human cells, but patients with mutated ZFP57 lack DNA binding capacity in in vitro EMSA studies (Baglivo et al. 2013).

There are significantly fewer ZFP57 sequence motifs in the placental-specific DMRs compared to the ubiquitous DMRs that inherit methylation from the germline ($P < 0.05$, Student's *t*-test), with 14/17 placental-specific DMRs being unmethylated and not associated with H3K9me3 in hES cells (Supplemental Fig. S10). These data further support our hypothesis that a novel imprinting mechanism occurs in the placenta, which is one of the first examples of methylation-independent epigenetic inheritance in mammals. In support of our observations, Park and colleagues (Park et al. 2004) generated a *H19* ICR knock-in at the *Afp* locus which was de novo methylated around gastrulation, implying that *H19* ICR is differentially marked in the gametes by a mechanism other than methylation. However, it is unknown if this mechanism also occurs at the endogenous *H19* locus. In our examples of placental-specific DMRs, the epigenetic mark inherited from the oocyte is currently unknown, but must be recognized by the de novo methylation machinery during early trophoblast differentiation, since we observe maternal methylation in term placenta. Certain histone methylation states are reported to recruit DNMTs (Dhayalan et al. 2010; Zhang et al. 2010). Since various post-translational modifications of histone tails have been shown to be present at imprinted loci, specifically in the placenta independent of DNA methylation (Umlauf et al. 2004; Monk et al. 2006), we are led to suggest one inviting hypothesis: A histone modification confers the "imprint" at these novel placental-specific imprinted loci. Alternatively, the DNMTs may be recruited to these loci by a specific, yet to be identified, transcription factor expressed during early trophoblast differentiation.

In line with other well-characterized imprinted genes in the placenta, the placental-specific imprinted transcripts may also exert supply-and-demand forces between the developing fetus and mother, ultimately influencing fetal adaptation in utero, which if disrupted may have long-term consequences on health many decades after delivery (Constância et al. 2004). Our observation of imprinting of the somatic promoter of *DNMT1* in placenta may therefore assist in this process. In addition, numerous studies have also suggested that children born as a result of assisted reproductive technologies (ART), including ovarian stimulation, in vitro fertilization, and intra-cytoplasmic sperm injections, have a higher risk of diseases with epigenetic etiologies, including imprinting disorders (Amor and Halliday 2008). In a clinical context, the placenta-specific imprinted loci may be prone to epigenetic instability during ART, as the first differentiation step that results in the trophectoderm occurs when the developing blastocysts are in culture.

By utilizing genome-wide methylation profiling at base-pair resolution, we have catalogued regions of parentally inherited methylation associated with imprinted regions and highlighted all differences between somatic and placental tissues. Further studies of these loci will provide insight into the causes of epigenetic ab-

Figure 5. Methylation in gametes, hES cells, and somatic tissues. (*A*) Heat maps for Infinium probes mapping within all ubiquitous (*left*) and placental-specific (*right*) imprinted DMRs in sperm and phES cells reveal the germline acquisition of methylation. (*B*) Methylation contour plots from WGBS data sets for all maternally methylated DMRs reveal that the extent of the intermediately methylated regions associated with imprinted DMRs are extremely consistent between somatic tissues and significantly larger in sperm. (*C*) Methylation profiles at the *NNAT* DMR determined by WGBS, Infinium array, and meDIP-seq data sets in leukocytes, sperm, phES cells, and hES cells, along with the H3K4me3 ChIP-seq reads for hES cells and sperm. The gray and black dots in the second panel represent Infinium probe methylation in hES cell lines derived from six-cell blastomeres (Val10B) and blastocytes (SHEF5), respectively. The gametic WGBS methylation profile is derived from sperm, with Infinium probe methylation values for sperm and phES cells represented by blue and red dots. The graphic shows the extent of the differentially methylated regions in somatic tissues and between sperm and phES cells. The error bars associated with the Infinium array probes represent the standard deviation of the two sperm samples and four independent phES cell lines. The H3K4me3 ChIP-seq data is from sperm. The methylation profiles were confirmed using standard bisulfite PCR and sequencing.

errations associated with imprinting disorders and may be relevant to the epigenetic causes of common diseases.

Methods

Tissue samples and cell lines

Peripheral blood was obtained from healthy volunteers or from the umbilical cord of newborns for which we obtained matched placental biopsies. These samples were collected at the Hospital St. Joan De Deu (Barcelona, Spain) and the National Center for Child Health and Development (Tokyo, Japan). All placenta-derived DNA samples were free of maternal DNA contamination based on microsatellite repeat analysis. The brain samples were obtained from BrainNet Europe/Barcelona Brain Bank. Ethical approval for this study was granted by the Institutional Review Boards at the National Center for Child Health and Development (project 234), Saga University (21-5), Hamamatsu University School of Medicine (23-12), Hospital St. Joan De Deu Ethics Committee (35/07), and Bellvitge Institute for Biomedical Research (PR006/08). Written informed consent was obtained from all participants.

The hES (SHEF 3, 5, 6 and Val10B) and parthenogenetically activated oocyte (LLC6P, LLC7P, LLC8P, and LLC9P) cell lines were used because they were epigenetically stable at imprinted loci (with the exception of *NNAT* LOM and *GNAS* GOM in LLC7P; LOM of *PEG3* in Val10B; GOM of *MCTS2P* in SHEF3) and grown as previously described (Harness et al. 2011). Ethical approval for the study of these cells was granted by the Bellvitge Institute for Biomedical Research Ethics Committee (PR096/10) and Comité Ético de Investigación Clínica (CEIC) del Centro de Medicina Regenerativa de Barcelona-CMR[B] (28/2012) and complied with the legal guidelines outlined by the Generalitat de Catalunya El conseller de Slaut.

Wild-type mouse embryos and placentae were produced by crossing C57BL/6 (B) with *Mus musculus molosinus* (JF1) or *Mus musculus castaneous* (C) mice. Mouse work was approved by the Institutional Review Board Committees at the National Center for Child Health and Development (approval number A2010-002). Animal husbandry and breeding were conducted according to the institutional guidelines for the care and the use of laboratory animals. DNA and RNA extractions and cDNA synthesis were carried out as previously described (Monk et al. 2006).

Characterization of the genome-wide UPD samples

Genomic DNA was isolated from two previously described genome-wide paternal UPD cases with BWS features (Romanelli et al. 2011) and two newly identified individuals, at Saga University, as well as one genome-wide maternal UPD with a SRS phenotype (Yamazawa et al. 2010). Each of these cases had undergone extensive molecular characterization to confirm genome-wide UPD status and the extent of mosaicism. We used DNA isolated from lymphocytes, as these samples had minimal contamination of the biparental cell lines. The genome-wide pUPD samples had 9, 11, 9, and 2% biparental contribution, whereas the genome-wide SRS sample had 16%. In addition, four hydatidiform moles were collected by the National Center for Child Health and Development.

Genome-wide methylation profiling

We analyzed six publicly available methylomes, including those derived from CD4+ lymphocytes (GSE31263) (Heyn et al. 2012), brain (GSM913595) (Zeng et al. 2012), the H1 hES cell line (GSM432685, GSM432686, GSM429321, GSM429322, GSM429323), and sperm (GSE30340). In addition, we generated three additional tissue methylomes using WGBS for brain, liver, and placenta. WGBS libraries were generated as previously described (Heyn et al. 2012).

We also generated methylation data sets using the Illumina Infinium HumanMethylation450 BeadChip arrays, which simultaneously quantifies ~2% of all CpG dinucleotides. Bisulfite conversion of 600 ng of DNA was performed according to the manufacturer's recommendations for the Illumina Infinium Assay (EZ DNA methylation kit, Zymo). The bisulfite-converted DNA was used for hybridization following the Illumina Infinium HD methylation protocol at genomic facilities of the Cancer Epigenetics and Biology Program (Barcelona, Spain) or the National Center for Child Health and Development. Data was generated for the genome-wide UPDs (4× pUPD, 1× mUPD), two brain, one liver, one muscle, one pancreas, two sperm, four hydatidiform moles, four term placentae, four phES cell lines, and the four hES lines. In addition, we used three leukocyte data sets from GSE30870.

Data filtering and analysis

For WGBS, the sequence reads were aligned to either strand of the hg19 reference genome using a custom computational pipeline (autosomal CpGs with at least five reads: brain sample, 190,314,071 aligned unique reads, 83% coverage; liver sample, 778,733,789 aligned unique reads, 96.6% coverage; placenta sample, 319,362,653 aligned unique reads, 89.6% coverage). The methylation level of each cytosine within CpG dinucleotides was estimated as the number of reads reporting a C, divided by the total number of reads reporting a C or T. For the identification of intermediately methylated regions associated with imprinted DMRs, we performed a sliding window approach in which the methylation of 25 CpGs was averaged after filtering for repetitive sequences. The location of these sequences was taken from the UCSC sequence browser. An interval was considered partially methylated if the average methylation was $0.25 < \text{mean} \pm 1.5\ \text{SD} < 0.75$.

For the Illumina Infinium HumanMethylation 450 BeadChip array, before analyzing the data, we excluded possible sources of technical biases that could influence results. We applied signal background subtraction, and inter-plate variation was normalized using default control probes in BeadStudio (version 2011.1_Infinium HD). We discarded probes with a detection *P*-value >0.01. We also excluded probes that lacked signal values in one or more of the DNA samples analyzed. In addition, we discarded 16,631 probes as they contained SNPs present in >1% of the population (dbSNP 137). Lastly, prior to screening for novel imprinted DMRs, we excluded all X chromosome CpG sites. In total, we analyzed 442,772 probes in all DNA samples. All hierarchical clustering and β-value evaluation was performed using the Cluster Analysis tool of the BeadStudio software.

In-house R-package scripts were used to evaluate the average methylation of three contiguous Infinium probes. To identify regions with potential allelic methylation, we screened the reciprocal genome-wide UPDs for three consecutive probes with an average β-value difference greater than 0.3 (Limma linear model $P < 0.05$):

$$\left|\frac{1}{3}\sum_{n=0}^{2} pUPDs_n - \frac{1}{3}\sum_{n=0}^{2} mUPD_n\right| > 0.3.$$

With the condition that the average of three consecutive probes for the normal leukocytes is between the values for the reciprocal genome-wide UPDs:

$$\begin{cases} if \frac{1}{3}\sum_{n=0}^{2} pUPDs_n > \frac{1}{3}\sum_{n=0}^{2} mUPD_n \\ then \frac{1}{3}\sum_{n=0}^{2} pUPDs_n > \frac{1}{3}\sum_{n=0}^{2} Leukocytes_n > \frac{1}{3}\sum_{n=0}^{2} mUPD_n \\ if \frac{1}{3}\sum_{n=0}^{2} mUPD_n > \frac{1}{3}\sum_{n=0}^{2} pUPDs_n \\ then \frac{1}{3}\sum_{n=0}^{2} mUPD_n > \frac{1}{3}\sum_{n=0}^{2} Leukocytes_n > \frac{1}{3}\sum_{n=0}^{2} pUPDs_n. \end{cases}$$

The final condition was that the average of three consecutive probes for normal leukocytes is within the 0.25–0.75 intermediate methylation range:

$$0.25 > \frac{1}{3}\sum_{n=0}^{2} Leukocytes_n > 0.75.$$

Genotyping and imprinting analysis

Genotypes of potential SNPs identified in the UCSC Genome Browser (hg19) were obtained by PCR and direct sequencing. Sequence traces were interrogated using Sequencher v4.6 (Gene Codes Corporation) to distinguish heterozygous and homozygous samples. Heterozygous sample sets were analyzed for either allelic expression using RT-PCR or bisulfite PCR, incorporating the polymorphism within the final PCR amplicon so that parental alleles could be distinguished (for primer sequence, see Supplemental Table S3).

Bisulfite PCR

Approximately 1 μg DNA was subjected to sodium bisulfite treatment and purified using the EZ DNA Methylation-Gold kit (Zymo), and was used for all bisulfite PCR analysis. Approximately 2 μL of bisulfite-converted DNA was used in each amplification reaction using Immolase Taq polymerase (Bioline) at 35–45 cycles, and the resulting PCR product cloned into pGEM-T easy vector (Promega) for subsequent subcloning and sequencing (for primer sequence, see Supplemental Table S3). For the confirmation of an imprinted DMR, we analyzed a minimum of three heterozygous samples and, where possible, two different tissues.

Chromatin immunoprecipitation (ChIP)

We analyzed publicly available H3K4me3 ChIP-seq and meDIP-seq data sets, including those derived from lymphocytes (GSM772948, GSM772836, GSM772916, GSM543025, GSM613913), brain (GSM806943, GSM806935, GSM806948, GSM669614, GSM669615), and the H1 hES cell line (GSM409308, GSM469971, GSM605315, GSM428289, GSM456941, GSM543016). For H3K9me3 in hES cells, we used GSM450266. In addition, we used the sperm ChIP-seq data set for H3K4me3 as a direct measure of nucleosome occupancy (GSM392696, GSM392697, GSM392698, GSM392714, GSM392715, GSM392716) (Hammoud et al. 2009).

The confirmation of allelic H3K4me3 in leukocytes or lymphoblastoid cell lines was performed as previously described (Iglesias-Platas et al. 2013). Briefly, 100 μg of chromatin was used for an immunoprecipitation reaction with Protein A agarose/salmon sperm DNA (16-157, Millipore) and a H3K4me3 (07-473, Millipore). Each ChIP was performed in triplicate alongside a mock immunoprecipitation with an unrelated IgG antiserum, and a 1% fraction of the input chromatin was extracted in parallel. Levels of immunoprecipitated chromatin at each specific region were determined by qPCR using SYBR Green (Applied Biosystems) carried out on the Applied Biosystems 7900 Fast real-time PCR system (for primer sequence, see Supplemental Table S3). Each PCR was run in triplicate and protein binding was quantified as a percentage of total input material.

Data access

The data from this study have been submitted to the NCBI Gene Expression Omnibus (GEO; http://www.ncbi.nlm.nih.gov/geo/) under accession number GSE52578.

List of affiliations

[1]Imprinting and Cancer Group, Cancer Epigenetic and Biology Program, Institut d'Investigació Biomedica de Bellvitge, Hospital Duran i Reynals, 08908 Barcelona, Spain; [2]Department of Maternal-Fetal Biology, National Research Institute for Child Health and Development, Tokyo 157-8535, Japan; [3]Servicio de Neonatología, Hospital Sant Joan de Déu, Fundació Sant Joan de Déu, 08950 Barcelona, Spain; [4]Department of Systems Biomedicine, National Research Institute for Child Health and Development, Tokyo 157-8535, Japan; [5]Fundación IVI-Instituto Universitario IVI-Universidad de Valencia, INCLIVA, 46980 Paterna, Valencia, Spain; [6]Centre for Stem Cell Biology, Department of Biomedical Science, University of Sheffield, Sheffield S10 2TN, United Kingdom; [7]Reeve-Irvine Research Centre, Sue and Bill Gross Stem Cell Research Center, Department of Anatomy and Neurobiology, School of Medicine, University of California at Irvine, Irvine, California 92697, USA; [8]Cancer Epigenetics Group, Cancer Epigenetic and Biology Program, Institut d'Investigació Biomedica de Bellvitge, Hospital Duran i Reynals, 08908 Barcelona, Spain; [9]Department of Obstetrics and Gynecology, Graduate School of Medical Science, Kyushu University, Fukuoka 812-8582, Japan; [10]Instituto de Genética Médica y Molecular, CIBERER, IDIPAZ-Hospital Universitario La Paz, Universidad Autónoma de Madrid, 28046 Madrid, Spain; [11]Division of Molecular Genetics and Epigenetics, Department of Biomolecular Sciences, Faculty of Medicine, Saga University, Saga 849-8501, Japan; [12]Department of Physiological Sciences II, School of Medicine, University of Barcelona, 08036 Barcelona, Catalonia, Spain; [13]Institucio Catalana de Recerca i Estudis Avançats (ICREA), 08010 Barcelona, Catalonia, Spain; [14]Department of Pediatrics, Hamamatsu University School of Medicine, Hamamatsu 431-3192, Japan.

Acknowledgments

We thank S. Morán at PEBC-IDIBELL for performing the methylation array hybridization and S. Sayols and H. Heyn for bioinformatics assistance. We also thank P. Arnaud and J. Frost for stimulating discussions and helpful comments. This work was partially funded by grants from the Fundació La Marató de TV3 (grant no. 101130 to D.M. and P.L.); Spanish Ministerio de Educacion y Ciencia (BFU2011-27658 to D.M.); JST/CREST and the Health and Labour Sciences Research Grant (Nanbyo-Ippan-003 to K.H.); the Ministry of Education, Culture, Sports, Science, and Technology of Japan (#22249010) and the National Center for Child Health and Development (#24-3) to K.N. D.M. is a Ramon y Cajal research fellow. Finally, we would like to thank all the patients and their families for participating in this project.

References

Amor DJ, Halliday J. 2008. A review of known imprinting syndromes and their association with assisted reproduction technologies. *Hum Reprod* **23:** 2826–2834.

Baglivo I, Esposito S, De Cesare L, Sparago A, Anvar Z, Riso V, Cammisa M, Fattorusso R, Grimaldi G, Riccio A, et al. 2013. Genetic and epigenetic mutations affect the DNA binding capability of human ZFP57 in transient neonatal diabetes type 1. *FEBS Lett* **587:** 1474–1481.
Barbaux S, Gascoin-Lachambre G, Buffat C, Monnier P, Mondon F, Tonanny MB, Pinard A, Auer J, Bessières B, Barlier A, et al. 2012. A genome-wide approach reveals novel imprinted genes expressed in the human placenta. *Epigenetics* **7:** 1079–1090.
Bourc'his D, Xu GL, Lin CS, Bollman B, Bestor TH. 2001. Dnmt3L and the establishment of maternal genomic imprints. *Science* **294:** 2536–2539.
Buiting K. 2010. Prader-Willi syndrome and Angelman syndrome. *Am J Med Genet C Semin Med Genet* **154C:** 365–376.
Choufani S, Shuman C, Weksberg R. 2010. Beckwith-Wiedemann syndrome. *Am J Med Genet C Semin Med Genet* **154C:** 343–354.
Ciccone DN, Su H, Hevi S, Gay F, Lei H, Bajko J, Xu G, Li E, Chen T. 2009. KDM1B is a histone H3K4 demethylase required to establish maternal genomic imprints. *Nature* **461:** 415–418.
Constância M, Kelsey G, Reik W. 2004. Resourceful imprinting. *Nature* **432:** 53–57.
Coombes C, Arnaud P, Gordon E, Dean W, Coar EA, Williamson CM, Feil R, Peters J, Kelsey G. 2003. Epigenetic properties and identification of an imprint mark in the Nesp-Gnasxl domain of the mouse *Gnas* imprinted locus. *Mol Cell Biol* **23:** 5475–5488.
Cooper WN, Constância M. 2010. How genome-wide approaches can be used to unravel the remaining secrets of the imprintome. *Brief Funct Genomics* **9:** 315–328.
Das R, Lee YK, Strogantsev R, Jin S, Lim YC, Ng PY, Lin XM, Chng K, Yeo GSh, Ferguson-Smith AC, et al. 2013. DNMT1 and AIM1 imprinting in human placenta revealed through a genome-wide screen for allele-specific DNA methylation. *BMC Genomics* **14:** 685.
Dhayalan A, Rajavelu A, Rathert P, Tamas R, Jurkowska RZ, Ragozin S, Jeltsch A. 2010. The Dnmt3a PWWP domain reads histone 3 lysine 36 trimethylation and guides DNA methylation. *J Biol Chem* **285:** 26114–26120.
Eggermann T. 2010. Russell-Silver syndrome. *Am J Med Genet C Semin Med Genet* **154C:** 355–364.
Ehrlich M, Gama-Sosa MA, Huang LH, Midgett RM, Kuo KC, McCune RA, Gehrke C. 1982. Amount and distribution of 5-methylcytosine in human DNA from different types of tissues of cells. *Nucleic Acids Res* **10:** 2709–2721.
El-Maarri O, Buiting K, Peery EG, Kroisel PM, Balaban B, Wagner K, Urman B, Heyd J, Lich C, Brannan CI, et al. 2001. Maternal methylation imprints on human chromosome 15 are established during or after fertilization. *Nat Genet* **27:** 41–44.
Fuke C, Shimabukuro M, Petronis A, Sugimoto J, Oda T, Miura K, Miyazaki T, Ogura C, Okazaki Y, Jinno Y. 2004. Age related changes in 5-methylcytosine content in human peripheral leukocytes and placentas: An HPLC-based study. *Ann Hum Genet* **68:** 196–204.
Geuns E, De Temmerman N, Hilven P, Van Steirteghem A, Liebaers I, De Rycke M. 2007. Methylation analysis of the intergenic differentially methylated region of DLK1-GTL2 in human. *Eur J Hum Genet* **15:** 352–361.
Gregg C, Zhang J, Weissbourd B, Luo S, Schroth GP, Haig D, Dulac C. 2010. High-resolution analysis of parent-of-origin allelic expression in the mouse brain. *Science* **329:** 643–648.
Hammoud SS, Nix DA, Zhang H, Purwar J, Carrell DT, Cairns BR. 2009. Distinctive chromatin in human sperm packages genes for embryo development. *Nature* **460:** 473–478.
Harness JV, Turovets NA, Seiler MJ, Nistor G, Altun G, Agapova LS, Ferguson D, Laurent LC, Loring JF, Keirstead HS. 2011. Equivalence of conventionally-derived and parthenote-derived human embryonic stem cells. *PLoS ONE* **6:** e14499.
Hata K, Okano M, Lei H, Li E. 2002. Dnmt3L cooperates with the Dnmt3 family of de novo DNA methyltransferases to establish maternal imprints in mice. *Development* **129:** 1983–1993.
Hayashizaki Y, Shibata H, Hirotsune S, Sugino H, Okazaki Y, Sasaki N, Hirose K, Imoto H, Okuizumi H, Muramatsu M, et al. 1994. Identification of an imprinted U2af binding protein related sequence on mouse chromosome 11 using the RLGS method. *Nat Genet* **6:** 33–40.
Heyn H, Li N, Ferreira HJ, Moran S, Pisano DG, Gomez A, Diez J, Sanchez-Mut JV, Setien F, Carmona FJ, et al. 2012. Distinct DNA methylomes of newborns and centenarians. *Proc Natl Acad Sci* **109:** 10522–10527.
Hiura H, Sugawara A, Ogawa H, John RM, Miyauchi N, Miyanari Y, Horiike T, Li Y, Yaegashi N, Sasaki H, et al. 2010. A tripartite paternally methylated region within the *Gpr1-Zdbf2* imprinted domain on mouse chromosome 1 identified by meDIP-on-chip. *Nucleic Acids Res* **38:** 4929–4945.
Kanber D, Berulava T, Ammerpohl O, Mitter D, Richter J, Siebert R, Horsthemke B, Lohman D, Buiting K. 2009. The human retinoblastoma gene is imprinted. *PLoS Genet* **12:** e1000790.
Iglesias-Platas I, Court F, Camprubi C, Sparago A, Guillaumet-Adkins A, Martin-Trujillo A, Riccio A, Moore GE, Monk D. 2013. Imprinting at the *PLAGL1* domain is contained within a 70-kb CTCF/cohesin-mediated non-allelic chromatin loop. *Nucleic Acids Res* **41:** 2171–2179.
Kagami M, Sekita Y, Nishimura G, Irie M, Kato F, Okada M, Yamamori S, Kishimoto H, Nakayama M, Tanaka Y, et al. 2008. Deletions and epimutations affecting the human 14q32.2 imprinted region in individuals with paternal and maternal upd(14)-like phenotypes. *Nat Genet* **40:** 237–242.
Kagami M, O'Sullivan MJ, Green AJ, Watabe Y, Arisaka O, Masawa N, Matsuoka K, Fukami M, Matsubara K, Kato F, et al. 2010. The IG-DMR and the *MEG3*-DMR at human chromosome 14q32.2: Hierarchical interaction and distinct functional properties as imprinting control centers. *PLoS Genet* **6:** e1000992.
Kelsey G. 2010. Imprinting on chromosome 20: Tissue-specific imprinting and imprinting mutations in the GNAS locus. *Am J Med Genet C Semin Med Genet* **154C:** 377–386.
Kelsey G, Bodle D, Miller HJ, Beechey CV, Coombes C, Peters J, Williamson CM. 1999. Identification of imprinted loci by methylation-sensitive representational difference analysis: Application to mouse distal chromosome 2. *Genomics* **62:** 129–138.
Kobayashi H, Sakurai T, Imai M, Takahashi N, Fukuda A, Yayoi O, Sato S, Nakabayashi K, Hata K, Sotomaru Y, et al. 2012. Contribution of intragenic DNA methylation in mouse gametic DNA methylomes to establish oocyte-specific heritable marks. *PLoS Genet* **8:** e1002440.
Kobayashi H, Yanagisawa E, Sakashita A, Sugawara N, Kumakura S, Ogawa H, Akutsu H, Hata K, Nakabayashi K, Kono T. 2013. Epigenetic and transcriptional features of the novel human imprinted lncRNA *GPR1AS* suggest it is a functional ortholog to mouse *Zdbf2linc*. *Epigenetics* **8:** 635–645.
Kong A, Steinthorsdottir V, Masson G, Thorleifsson G, Sulem P, Besenbacher S, Jonasdottir A, Sigurdsson A, Kristinsson KT, Jonasdottir A, et al. 2009. Parental origin of sequence variants associated with complex diseases. *Nature* **462:** 868–874.
Lapunzina P, Monk D. 2011. The consequences of uniparental disomy and copy number neutral loss-of-heterozygosity during human development and cancer. *Biol Cell* **103:** 303–317.
Li X, Ito M, Zhou F, Youngson N, Zuo X, Leder P, Ferguson-Smith AC. 2008. A maternal-zygotic effect gene, *Zfp57*, maintains both maternal and paternal imprints. *Dev Cell* **15:** 547–557.
Lister R, Pelizzola M, Dowen RH, Hawkins RD, Hon G, Tonti-Filippini J, Nery JR, Lee L, Ye Z, Ngo QM, et al. 2009. Human DNA methylomes at base resolution show widespread epigenomic differences. *Nature* **462:** 315–322.
Lopes S, Lewis A, Hajkova P, Dean W, Oswald J, Forné T, Murrell A, Constância M, Bartolomei M, Walter J, et al. 2003. Epigenetic modifications in an imprinting cluster are controlled by a hierarchy of DMRs suggesting long-range chromatin interactions. *Hum Mol Genet* **12:** 295–305.
Mackay DJ, Temple IK. 2010. Transient neonatal diabetes mellitus type 1. *Am J Med Genet C Semin Med Genet* **154C:** 335–342.
Mai Q, Yu Y, Li T, Wang L, Chen MJ, Huang SZ, Zhou C, Zhou Q. 2007. Derivation of human embryonic stem cell lines from parthenogenetic blastocysts. *Cell Res* **17:** 1008–1012.
Molaro A, Hodges E, Fang F, Song Q, McCombie WR, Hannon GJ, Smith AD. 2011. Sperm methylation profiles reveal features of epigenetic inheritance and evolution in primates. *Cell* **146:** 1029–1041.
Monk D. 2010. Deciphering the cancer imprintome. *Brief Funct Genomics* **9:** 329–339.
Monk D, Arnaud P, Apostolidou S, Hills FA, Kelsey G, Stanier P, Feil R, Moore GE. 2006. Limited evolutionary conservation of imprinting in the human placenta. *Proc Natl Acad Sci* **103:** 6623–6628.
Nakabayashi K, Trujillo AM, Tayama C, Camprubi C, Yoshida W, Lapunzina P, Sanchez A, Soejima H, Aburatani H, Nagae G, et al. 2011. Methylation screening of reciprocal genome-wide UPDs identifies novel human-specific imprinted genes. *Hum Mol Genet* **20:** 3188–3197.
Nakamura T, Arai Y, Umehara H, Masuhara M, Kimura T, Taniguchi H, Sekimoto T, Ikawa M, Yoneda Y, Okabe M. 2007. PGC7/Stella protects against DNA demethylation in early embryogenesis. *Nat Cell Biol* **9:** 64–71.
Noguer-Dance M, Abu-Amero S, Al-Khtib M, Lefèvre A, Coullin P, Moore GE, Cavaillé J. 2010. The primate-specific microRNA gene cluster (C19MC) is imprinted in the placenta. *Hum Mol Genet* **19:** 3566–3582.
Okae H, Hiura H, Nishida Y, Funayama R, Tanaka S, Chiba H, Yaegashi N, Nakayama K, Sasaki H, Arima T. 2011. Re-investigation and RNA sequencing-based identification of genes with placenta-specific imprinted expression. *Hum Mol Genet* **21:** 548–558.
Park KY, Sellars EA, Grinberg A, Huang SP, Pfeifer K. 2004. The H19 differentially methylated region marks the parental origin of a heterologous locus without gametic DNA methylation. *Mol Cell Biol* **24:** 3588–3595.
Proudhon C, Duffié R, Ajjan S, Cowley M, Iranzo J, Carbajosa G, Saadeh H, Holland ML, Oakey RJ, Rakyan VK, et al. 2012. Protection against de

novo methylation is instrumental in maintaining parent-of-origin methylation inherited from the gametes. *Mol Cell* **47:** 909–920.
Quenneville S, Verde G, Corsinotti A, Kapopoulou A, Jakobsson J, Offner S, Baglivo I, Pedone PV, Grimaldi G, Riccio A, et al. 2011. In embryonic stem cells, ZFP57/KAP1 recognize a methylated hexanucleotide to affect chromatin and DNA methylation of imprinting control regions. *Mol Cell* **44:** 361–372.
Ramowitz LK, Bartolomei MS. 2011. Genomic imprinting: Recognition and marking of imprinted loci. *Curr Opin Genet Dev* **22:** 72–78.
Romanelli V, Nevado J, Fraga M, Trujillo AM, Mori MÁ, Fernández L, Pérez de Nanclares G, Martínez-Glez V, Pita G, Meneses H, et al. 2011. Constitutional mosaic genome-wide uniparental disomy due to diploidisation: An unusual cancer-predisposing mechanism. *J Med Genet* **48:** 212–216.
Schroeder DI, Blair JD, Lott P, Yu HO, Hong D, Crary F, Ashwood P, Walker C, Korf I, Robinson WP, et al. 2013. The human placenta methylome. *Proc Natl Acad Sci* **110:** 6037–6042.
Sharp A, Migliavacca E, Dupre Y, Stathaki E, Reza Sailani M, Baumer A, Schinzel A, Mackay DJ, Robinson DO, Cobellis G, et al. 2010. Methylation profiling in individuals with uniparental disomy identify novel differentially methylated regions on chromosome 15. *Genome Res* **20:** 1271–1278.
Smallwood SA, Tomizawa S, Krueger F, Ruf N, Carli N, Segonds-Pichon A, Sato S, Hata K, Andrews SR, Kelsey G. 2011. Dynamic CpG island methylation landscape in oocytes and pre-implantation embryos. *Nat Genet* **43:** 811–814.
Smith ZD, Chan MM, Mikkelsen TS, Gu H, Gnirke A, Regev A, Meissner A. 2012. A unique regulatory phase of DNA methylation in the early mammalian embryo. *Nature* **484:** 339–344.
Thomson JP, Skene PJ, Selfridge J, Clouaire T, Guy J, Webb S, Kerr AR, Deaton A, Andrews R, James KD, et al. 2010. CpG islands influence chromatin structure via the CpG-binding protein Cfp1. *Nature* **464:** 1082–1086.
Tomizawa S, Kobayashi H, Watanabe T, Andrews S, Hata K, Kelsey G, Sasaki H. 2011. Dynamic stage-specific changes in imprinted differentially methylated regions during early mammalian development and prevalence of non-CpG methylation in oocytes. *Development* **138:** 811–820.
Umlauf D, Goto Y, Cao R, Cerqueira F, Wagschal A, Zhang Y, Feil R. 2004. Imprinting along the *Kcnq1* domain on mouse chromosome 7 involves repressive histone methylation and recruitment of Polycomb group complexes. *Nat Genet* **36:** 1296–1300.
Wood AJ, Schulz R, Woodfine K, Koltowska K, Beechey CV, Peters J, Bourc'his D, Oakey RJ. 2008. Regulation of alternative polyadenylation by genomic imprinting. *Genes Dev* **22:** 1141–1146.
Xie W, Barr CL, Kim A, Yue F, Lee AY, Eubanks J, Dempster EL, Ren B. 2012. Base-resolution analyses of sequence and parent-of-origin dependent DNA methylation in the mouse genome. *Cell* **148:** 816–831.
Yamazawa K, Nakabayashi K, Kagami M, Sato T, Saitoh S, Horikawa R, Hizuka N, Ogata T. 2010. Parthenogenetic chimaerism/mosaicism with a Silver-Russell syndrome-like phenotype. *J Med Genet* **47:** 782–785.
Yuen RKC, Jiang R, Penaherrera M, McFadeen DE, Robinson WP. 2011. Genome-wide mapping of imprinted differentially methylated regions by DNA methylation profiling of human placentas from triploidies. *Epigenetics & Chromatin* **4:** 10.
Zeng J, Konopka G, Hunt BG, Preuss TM, Geschwind D, Yi SV. 2012. Divergent whole-genome methylation maps of human and chimpanzee brains reveal epigenetic basis of human regulatory evolution. *Am J Hum Genet* **91:** 455–465.
Zhang Y, Jurkowska R, Soeroes S, Rajavelu A, Dhayalan A, Bock I, Rathert P, Brandt O, Reinhardt R, Fischle W, et al. 2010. Chromatin methylation activity of Dnmt3a and Dnmt3a/3L is guided by interaction of the ADD domain with the histone H3 tail. *Nucleic Acids Res* **38:** 4246–4253.

Received August 9, 2013; accepted in revised form December 26, 2013.

CLINICAL GENETICS An International Journal of Genetics, Molecular and Personalized Medicine

Clin Genet 2013
Printed in Singapore. All rights reserved

Published by John Wiley & Sons Ltd
CLINICAL GENETICS
doi: 10.1111/cge.12318

Short Report

A novel *de novo* point mutation of the OCT-binding site in the *IGF2/H19*-imprinting control region in a Beckwith–Wiedemann syndrome patient

Higashimoto K, Jozaki K, Kosho T, Matsubara K, Fuke T, Yamada D, Yatsuki H, Maeda T, Ohtsuka Y, Nishioka K, Joh K, Koseki H, Ogata T, Soejima H. A novel *de novo* point mutation of the OCT-binding site in the *IGF2/H19*-imprinting control region in a Beckwith–Wiedemann syndrome patient.
Clin Genet 2013. © John Wiley & Sons A/S. Published by John Wiley & Sons Ltd, 2013

The *IGF2/H19*-imprinting control region (ICR1) functions as an insulator to methylation-sensitive binding of CTCF protein, and regulates imprinted expression of *IGF2* and *H19* in a parental origin-specific manner. ICR1 methylation defects cause abnormal expression of imprinted genes, leading to Beckwith–Wiedemann syndrome (BWS) or Silver–Russell syndrome (SRS). Not only ICR1 microdeletions involving the CTCF-binding site, but also point mutations and a small deletion of the OCT-binding site have been shown to trigger methylation defects in BWS. Here, mutational analysis of ICR1 in 11 BWS and 12 SRS patients with ICR1 methylation defects revealed a novel *de novo* point mutation of the OCT-binding site on the maternal allele in one BWS patient. In BWS, all reported mutations and the small deletion of the OCT-binding site, including our case, have occurred within repeat A2. These findings indicate that the OCT-binding site is important for maintaining an unmethylated status of maternal ICR1 in early embryogenesis.

Conflict of interest

The authors have no competing financial interests to declare.

K Higashimoto[a], K Jozaki[a], T Kosho[b], K Matsubara[c], T Fuke[c], D Yamada[d], H Yatsuki[a], T Maeda[a], Y Ohtsuka[a], K Nishioka[a], K Joh[a], H Koseki[d], T Ogata[e] and H Soejima[a]

[a]Division of Molecular Genetics & Epigenetics, Department of Biomolecular Sciences, Faculty of Medicine, Saga University, Saga, Japan, [b]Department of Medical Genetics, Shinshu University School of Medicine, Matsumoto, Nagano, Japan, [c]Department of Molecular Endocrinology, National Research Institute for Child Health and Development, Tokyo, Japan, [d]Laboratory for Developmental Genetics, RIKEN Center for Integrative Medical Sciences (IMS), Yokohama, Kanagawa, Japan, and [e]Department of Pediatrics, Hamamatsu University School of Medicine, Hamamatsu, Japan

Key words: Beckwith–Wiedemann syndrome – ICR1 methylation defect – *IGF2/H19* – OCT-binding site – Silver–Russell syndrome

Corresponding author: Hidenobu Soejima, Division of Molecular Genetics & Epigenetics, Department of Biomolecular Sciences, Faculty of Medicine, Saga University, 5-1-1 Nabeshima, Saga 849–8501, Japan.
Tel.: +81 952 34 2260;
fax: +81 952 34 2067;
e-mail: soejimah@cc.saga-u.ac.jp

Received 5 August 2013, revised and accepted for publication 6 November 2013

Human 11p15 contains two neighboring imprinted domains, *IGF2/H19* and *KCNQ1*. Each domain is controlled by its own imprinting control region: ICR1 or ICR2, respectively (1). ICR1 methylation defects cause abnormal imprinted expression of insulin-like growth factor 2 (*IGF2*), which encodes a growth factor, and non-coding RNA *H19*, which possesses possible tumor-suppressor functions, leading to Beckwith–Wiedemann syndrome (BWS: OMIM 130650) and Silver–Russell syndrome (SRS: OMIM 180860), respectively (1, 2).

BWS is a congenital overgrowth disorder characterized by macroglossia, macrosomia, and abdominal wall defects, whereas SRS is a congenital growth retardation disorder characterized by a typical facial gestalt, clinodactyly V, and body asymmetry (1, 2). Among varied causative genetic and epigenetic abnormalities, ICR1 methylation defects are etiologies common to both diseases. Gain of methylation (GOM) and loss of methylation (LOM) at ICR1 account for ~5% of BWS and ~44% of SRS cases, respectively (1, 2).

ICR1 upstream of *H19* is a differentially methylated region (DMR) that is methylated exclusively on the paternal allele, and it regulates the imprinted expression of paternally expressed *IGF2* and maternally expressed *H19*. On the maternal allele, unmethylated ICR1 bound by CTCF forms a chromatin insulator that prevents *IGF2* promoter activation by the enhancer downstream of *H19*, resulting in silencing of *IGF2* and activation of *H19*. On the paternal allele, methylation-sensitive CTCF cannot bind to methylated ICR1, resulting in activation of *IGF2* and silencing of *H19* (3, 4). CTCF also maintains the unmethylated status of ICR1 on the maternal allele (5, 6).

Human ICR1 contains two different repetitive sequences (A and B) and seven CTCF-binding sites (CTSs) (Fig. 1a). A maternally inherited ICR1 microdeletion (1.4–2.2 kb), which affects ICR1 function and CTCF binding by changing CTS spacing, has been reported to result in ICR1-GOM in a few familial BWS cases (7–9). ICR1 also contains other protein-binding motifs, such as OCT, SOX, and ZFP57 (10, 11). Recently, point mutations and a small deletion of the OCT or SOX motif have been reported in a few BWS patients with ICR1-GOM (10, 12, 13).

Here, mutational analysis in 11 BWS and 12 SRS patients with ICR1 methylation defects revealed a novel *de novo* point mutation in the OCT-binding site on the maternal allele of one BWS patient.

Materials and methods

Patients

Eleven BWS and twelve SRS patients, who were clinically diagnosed, were enrolled in this study. All BWS and SRS patients displayed isolated GOM and LOM of ICR1, respectively. This study was approved by the Ethics Committee for Human Genome and Gene Analyses of the Faculty of Medicine, Saga University. Written informed consents were obtained from the parents or guardians of the patients.

Sequencing analysis of ICR1

A genomic region in and around ICR1, which included seven CTSs and three OCT-binding sites, was directly sequenced in all patients as previously described (14). All polymerase chain reaction (PCR) primer pairs used are listed in Table S1, Supporting Information.

Microsatellite analysis

For quantitative polymorphism analysis, tetranucleotide repeat markers, *D11S1984* at 11p15.5 and *D11S1997* at 11p15.4, were amplified and analyzed with GeneMapper software. The peak height ratios of the paternal allele to the maternal allele were calculated.

Southern blot analysis

Methylation-sensitive Southern blots with *Pst*I/*Mlu*I and *Bam*HI/*Not*I were employed for ICR1 and ICR2, respectively, as described previously (15). Band intensity was measured using a FLA-7000 fluoro-image analyzer (Fujifilm, Tokyo, Japan). The methylation index (MI, %) was then calculated.

Bisulfite sequencing

Bisulfite sequencing was performed covering the three variants within ICR1 that were found in BWS-s043. Genomic DNA was bisulfite-converted using an EpiTect Bisulfite Kit (Qiagen, Hilden, Germany). After PCR amplification, the products were cloned and sequenced.

Electrophoretic mobility shift assay

The pCMX-Flag-human OCT4 and pCMX-Flag-human SOX2 were simultaneously transfected into HEK293 cells. The nuclear extracts from HEK293 cells expressing human OCT4/SOX2 and mouse ES cells were used. Electrophoretic mobility shift assay (EMSA) was performed as described previously (10). For supershift analysis, 1.5 μg of anti-OCT4 antibody (Abcam, ab19857, Cambridge, UK) or 1.5 μg of anti-SOX2 antibody (R&D systems, AF2018, Minneapolis, MN) was used. The unlabeled probes were also used as competitors. The reaction mixtures were separated on a 4% polyacrylamide gel and exposed to a film. Oligonucleotide sequences are presented in Table S1.

Results

Among 11 BWS and 12 SRS patients with ICR1 methylation defects, 7 and 2 variants from 5 BWS and 2 SRS patients were found, respectively (Table 1). The variants in BWS-047 and BWS-s061 were polymorphisms. The remaining variants were not found in the normal population, the UCSC Genome Browser database, or the 1000 Genomes database, suggesting them to be candidates for causative mutations for ICR1 methylation defects. However, the positions of the variants, except

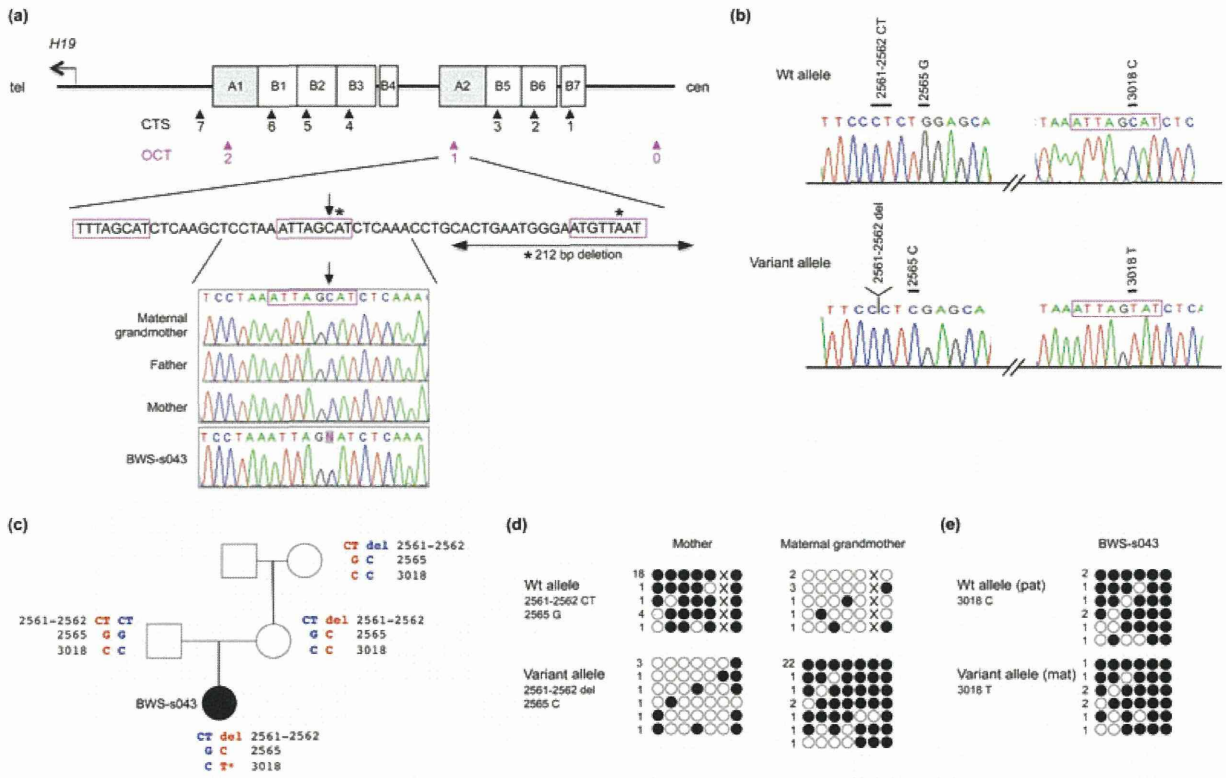

Fig. 1. The three variants in BWS-s043 and their effects on ICR1 methylation. (**a**) Map of ICR1 and the position of 2,023,018C>T. Upper panel: structure of ICR1. ICR1 consists of two repeat blocks. Each block consists of one repeat A and three or four repeat Bs. The black and red arrowheads indicate CTCF-binding sites (CTS) and OCT-binding sites (OCT), respectively. Middle panel: the position of 2,023,018C>T (arrow) and previously reported mutations and deletions (asterisks). Three octamer motifs are enclosed by a red line. Lower panel: electrophoretograms around 2,023,018C>T. BWS-s043 were heterozygous for the variant, whereas the maternal grandmother and both parents did not harbor it. (**b**) Haplotype encompassing the three variants in BWS-s043. Polymerase chain reaction (PCR) products encompassing the three variants were cloned and sequenced. All three variants were revealed to be on the same allele in BWS-s043. (**c**) Pedigree and haplotype of the family. Haplotype analysis showed that 2,023,018C>T (asterisk) occurred on the maternal allele in BWS-s043. (**d**) Bisulfite sequencing analysis encompassing the 2,022,561-562CT>delCT and the 2,022,565G>C variants in the mother and the maternal grandmother. Open and filled circles indicate unmethylated and methylated CpG sites, respectively. X indicates G at chr11: 2,022,565. Numerals on the left reflect the number of clones with the same methylation pattern. The variant allele was unmethylated in the mother and methylated in the maternal grandmother, respectively. (**e**) Bisulfite sequencing analysis encompassing 2,023,018C>T in BWS-s043. The maternal allele contained a *de novo* variant that was heavily methylated in BWS-s043, while differential methylation was maintained in other family members and normal controls without the variant (Fig. S2a).

Table 1. Variants found in this study[a]

Patient ID	MI of ICR1 (%)	Variant	Position (GRCh37/hg19 chr11)	Location	Transmission	Heterozygosity in normal population
BWS-047	100	G>Gdel	2,024,428	Centromeric outside of ICR1 (5′ of CTS1)	Maternal	2/116 (rs200288360)
		CT>CT del	2,022,561–2,022,562	Between A2 and B4	Maternal	na
BWS-s043	86	G>C	2,022,565	Between A2 and B4	Maternal	0/115
		C>T	2,023,018	A2 (OCT-binding site 1)	*De novo*	0/107
BWS-s061	76	C>T	2,023,497	B5 (5′ of CTS3)	Paternal	2/105
BWS-s081	67	C>T	2,025,777	Centromeric outside of ICR1 (3′ of OCT-binding site 0)	Paternal	0/106
BWS-s100	67	C>A	2,021,145	B1 (3′ of CTS6)	Maternal	0/105
SRS-002	4	G>Gdel	2,024,364	B7 (5′ of CTS1)	Unknown	0/106
SRS-s03	24	C>T	2,021,103	B1 (3′ of CTS6)	Maternal	0/106

ICR, imprinting control region; MI, methylation index; na, not analyzed.
[a]Parents' DNA were not available for SRS-002.

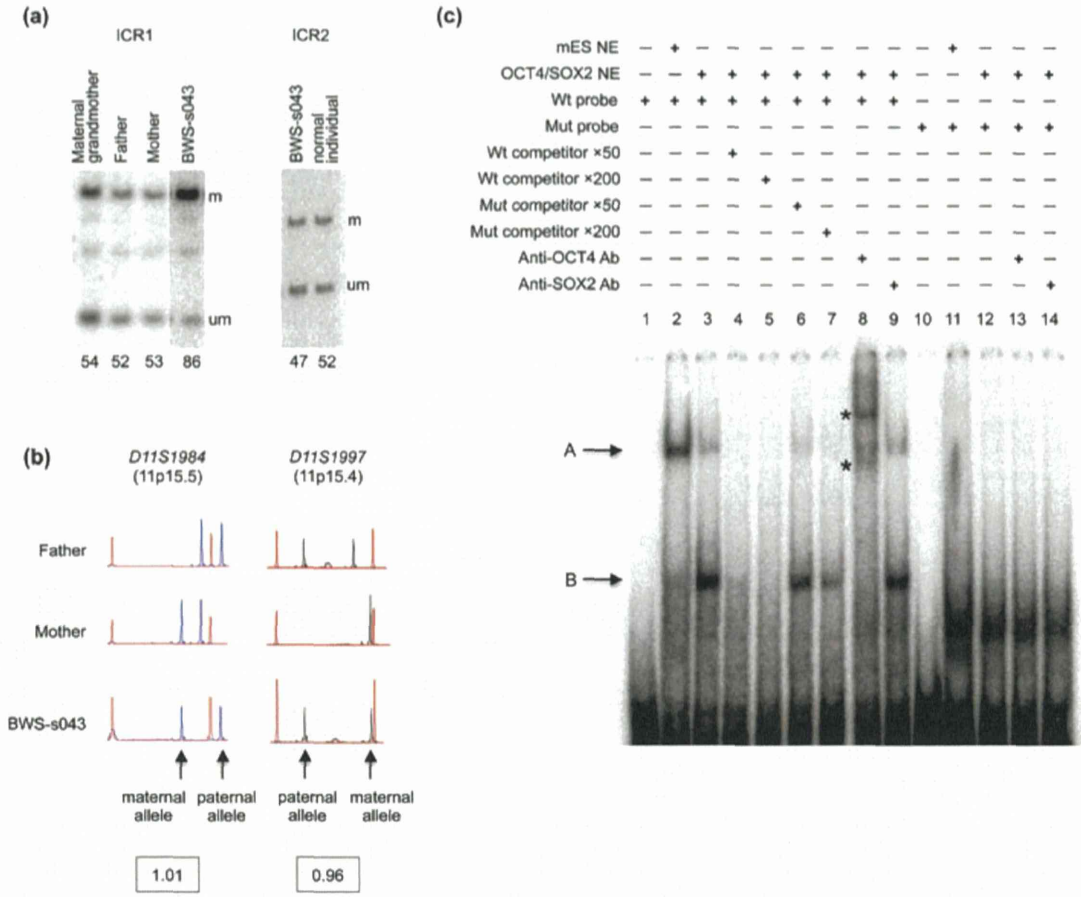

Fig. 2. Methylation-sensitive Southern blots and microsatellite analysis of BWS-s043, and electrophoretic mobility shift assay (EMSA) for 2,023,018C>T. (**a**) Methylation-sensitive Sothern blots of ICR1 and ICR2. Methylation indices [MI, %] are shown below each lane. MI was calculated using the equation $M/(M+U) \times 100$, where M is the intensity of the methylated band and U is the intensity of the unmethylated band. m, methylated band; um, unmethylated band. BWS-s043 showed ICR1-GOM, whereas the relatives did not. Methylation statuses of CTS1 and CTS4 are shown in Fig. S2b,c. Methylation of ICR2 in BWS-s043 was normal. (**b**) Microsatellite analysis at 11p15.4-p15.5. Ratios of the paternal allele to the maternal allele in BWS-s043 were approximately 1, indicating no uniparental disomy. Red peaks are molecular markers. (**c**) EMSA using the wild-type (Wt) probe and the mutant (Mut) probe encompassing 2,023,018C>T. The unlabeled Wt probe or Mut probe (×50 or ×200 molar excess) was used as a competitor. The arrows and asterisks indicate the protein-DNA complexes (A and B) and supershifted complexes, respectively. mES NE, nuclear extract from mouse ES cells; OCT4/SOX2 NE, nuclear extract from human HEK293 cells expressing OCT4/SOX2; Ab, antibody.

for BWS-s043, were not located at any protein-binding sites that have been reported as involved in methylation imprinting (CTCF, OCT, and ZFP57) (3, 4, 10, 12, 16). Furthermore, we did not find any protein-oligonucleotide complexes in EMSA using mouse ES nuclear extracts and oligonucleotide probes encompassing all variants, except for BWS-s043 (Fig. S1). Therefore, we analyzed further three variants in BWS-s043, which were in and around the OCT-binding site 1.

First, we re-confirmed that BWS-s043 showed GOM near CTS6 within ICR1, but it did not demonstrate LOM at ICR2, paternal uniparental disomy of chromosome 11, or a *CDKN1C* mutation (Fig. 2a,b, and data not shown). The 2,023,018C>T variant was located in the second octamer motif of OCT-binding site 1 within repeat A2 (Fig. 1a). The other two variants were located approximately 450 bp on the telomeric side of the 2,023,018C>T variant, between repeats A2 and B4 (Fig. 1a, Table 1). The 2,023,018C>T variant was absent in other family members, indicating a *de novo* variant (Fig. 1a). To clarify if the *de novo* variant in the patient occurred on the maternal or paternal allele, we performed haplotype analysis with PCR covering all three variants. We found all three variants were located on the same allele and the 2,023,018C>T variant occurred *de novo* on the maternal allele because the 2,022,561–562CT>delCT and 2,022,565G>C variants were on the maternal allele in the patient (Fig. 1b,c).

Next, we investigated the methylation status of ICR1. Methylation-sensitive Southern blots and bisulfite sequencing showed normal methylation of ICR1 in the parents and the maternal grandmother (Figs 2a and S2). As for the 2,022,561-562CT>delCT and the 2,022,565G>C variants, the variant allele was unmethylated in the mother, but methylated in the grandmother (Fig. 1d). On the basis of methylation